2009-01-01

Investigation of Polarization Dependent Loss for a Macrobending Loss Sensitive Singlemode Fiber

Pengfei Wang
Technological University Dublin, pengfei.wang@tudublin.ie

Gerald Farrell
Technological University Dublin, gerald.farrell@tudublin.ie

Yuliya Semenova
Technological University Dublin, yuliya.semenova@tudublin.ie

See next page for additional authors

Recommended Citation

Wang, P.et al (2009) Investigation of Polarization Dependent Loss for a Macrobending Loss Sensitive Singlemode Fiber. *Microwave and Optical Technology Letters,* Vol. 51, No. 6, pp. 1460-1464. DOI:10.1002/mop.24388

Authors
Pengfei Wang, Gerald Farrell, Yuliya Semenova, and Ginu Rajan

Investigation of Polarization Dependent Loss for a Macrobending Loss Sensitive Singlemode Fiber

Pengfei Wang, Gerald Farrell, Yuliya Semenova, Ginu Rajan

Applied Optoelectronics Center, School of Electronics and Communication Engineering, Dublin Institute of Technology, Kevin Street, Dublin 8, Ireland
pengfei.wang@student.dit.ie

Abstract: An investigation of the polarization dependent loss (PDL) of macrobending loss sensitive single fiber (1060XP) is presented theoretically and experimentally. The experimental results are in good agreement with the modeling outcomes. Through the comparison of experimental results of PDL between 1060XP fiber with coatings and bare 1060XP fiber, it is shown that the fiber coating has significant impact on the PDL of bend loss sensitive singlemode fiber.

Keywords: Polarization dependent loss, macrobending loss, singlemode fiber, 1060XP fiber

1. Introduction

PDL has been investigated as an important issue in many fiber-optic communication applications [1-4]. Polarization dependence is mostly caused by fiber bending, dichroism and oblique reflection, and it always increases the error rate in fiber-optic transmission systems. Recently, fiber macrobending loss of standard Corning SMF28 singlemode fiber was investigated theoretically and experimentally and was optimized as an all-fiber edge filter for a rapid wavelength measurement application [5]. Low polarization dependence in the macrobending loss transmission spectrum is a requirement for such an all-fiber ratiometric wavelength measurement system. However, the structure of an SMF28 fiber based edge filter is complex from a theoretical perspective for modeling and in addition an SMF28 fiber based filter requires a significant number of turns of fiber, for example, 22 turns with a bend radius of 11 mm [5], because SMF28 is bend loss insensitive. Therefore, the optimal design of a more compact fiber edge filter would benefit from using a bend loss sensitive singlemode fiber, and in [6], we proposed a bend loss sensitive singlemode fiber, 1060XP, for this purpose.

This paper presents the results of a thorough investigation of the PDL behavior of 1060XP fiber with different bend radii, including: 1) calculation of the correction factor of a bent 1060XP fiber with coating and absorbing layers; 2) theoretical modeling and PDL measurements of a bent 1060XP fiber, with coating and absorbing layers; 3) PDL measurements of bare bent 1060XP fiber with an absorbing layer. Through comparison of PDL results between 1060XP fiber with and without a coating, the fiber coating layer is shown to have significant effect on PDL performance.

2. Correction factor for bent 1060XP fiber with coating and absorbing layers

It is well known, when optical fiber is bent, that the presence of the coating layer(s) produces a so-called whispering-gallery mode due to the reflection of the radiated field at the interfaces of cladding-coating and coating-air layers. To reduce the whispering-gallery modes, the 1060XP fiber employed in this investigation is coated with an absorbing layer, and the fiber can thus be treated as a fiber core-cladding-infinite coating structure, as depicted in Fig. 1; where the *z*–axis is the direction of light propagation.

For 1060XP fiber, selected properties are listed in Table 1:

Following the weak-guidance approximation theory [7], when the fiber is bent, the Fourier transform scalar field in the cladding and infinite coating regions (q=2, 3) in y-direction can be expressed as:

$$\frac{d^2\overline{\psi}_q(x,\varsigma)}{dx^2}+\left[k^2n_q^2(1+\frac{2x}{R})-\beta_0^2-\varsigma^2\right]\overline{\psi}_q(x,\varsigma)=0 \qquad (1)$$

where ζ is the conjugate variable for the Fourier transform in y-direction. Following solution by an inverse Fourier transform of the y-field, formula (1) can be treated as [8]:

$$\psi_q(x,y)=\frac{1}{2\pi}\int_{-\infty}^{+\infty}\left[D_q(\varsigma)B_i(X_q)+H_q(\varsigma)A_i(X_q)\right]\cdot\exp(-i\varsigma y)d\varsigma \qquad (2)$$

where $X(x,\varsigma)=\left(\frac{R}{2k^2n_q^2}\right)^{2/3}\left[\beta^2+\varsigma^2-k^2n_q^2(1+\frac{2x}{R})\right]$, and B_i and A_i are Airy functions, respectively. For any two adjacent layers, given the continuous boundary conditions of the field, the adjacent fields for the TE mode (polarization direction is x-z direction in Fig. 1) is given by [9]:

$$\begin{cases} D_q(\zeta)B_i[X_q(x_q,\zeta)]+H_qA_i[X_q(x_q,\zeta)]=D_{q+1}(\zeta)B_i[X_q(x_{q+1},\zeta)]+H_{q+1}A_i[X_q(x_{q+1},\zeta)] \\ D_q(\zeta)B_i^{'}[X_q(x_q,\zeta)]+H_qA_i^{'}[X_q(x_q,\zeta)]=D_{q+1}(\zeta)B_i^{'}[X_q(x_{q+1},\zeta)]+H_{q+1}A_i^{'}[X_q(x_{q+1},\zeta)] \end{cases} \quad (3)$$

By solving the boundary condition using perturbation and scalar approximation theory, the bend loss coefficient of the TE mode, defined as α_{TE}, can be calculated.

In prior work [10, 11], an "effective bend radius" (R_{eff}) was introduced to fit the theoretically calculated bend losses to experimentally measured values. R_{eff} is related to the measured bend radius (R_{exp}) by a wavelength-dependent elasto-optic correction factor that accounts for the change in refractive index induced by axial bending stress [11]. Fig. 2 shows TE-mode bend loss results for 1060XP fiber coated with an absorbing layer (to remove reflections at the air-coating interface) measured when bend radius was systematically varied between 8.5 and 12.5 mm, at 1550 nm. Figure 2 also shows the theoretically calculated bend-loss values, both uncorrected (*i.e.*, R_{eff} = 1) and best-fit. Reasonable agreement between theoretical and experimental results is achieved with R_{eff}(1550 nm) = 1.283. Consequently, it is suggested that the correction factor of 1.283 at 1550 nm might be employed in the theoretical macrobending loss calculation of 1060XP fiber.

However, a bend loss based fiber edge filter is designed to cover a range of wavelengths. The correction factor varies with wavelength and while it is not practical to determine the value of the correction factor at all wavelengths, it was determined at 10 nm intervals over the wavelength range of interest between 1500 and 1600 nm. The correction factor as a function of wavelength is shown in Fig. 3.

3. Theoretical modeling and experiments for the PDL of a bent 1060XP fiber with coating and absorbing layers

To solve the different boundary conditions between the fiber's adjacent layers (q=2, 3), the adjacent fields for the TM mode (polarization direction is y-z direction in Fig. 1) can be expressed as following:

$$\begin{cases} D_q(\zeta)B_i[X_q(x_q,\zeta)]+H_qA_i[X_q(x_q,\zeta)]=D_{q+1}(\zeta)B_i[X_q(x_{q+1},\zeta)]+H_{q+1}A_i[X_q(x_{q+1},\zeta)] \\ \frac{1}{n_q^2}\left\{D_q(\zeta)B_i^{'}[X_q(x_q,\zeta)]+H_qA_i^{'}[X_q(x_q,\zeta)]\right\}=\frac{1}{n_{q+1}^2}\left\{D_{q+1}(\zeta)B_i^{'}[X_q(x_{q+1},\zeta)]+H_{q+1}A_i^{'}[X_q(x_{q+1},\zeta)]\right\} \end{cases} \quad (4)$$

Therefore, the bend loss coefficients, α_{TE} and α_{TM}, and the bend loss values, BL_{TE} and BL_{TM}, of the TE and TM modes can be calculated. To better characterize the polarization sensitivity of the bend loss, an absolute value of PDL can be defined by $PDL=\left|BL_{TE}-BL_{TM}\right|$. In our previous work [6], it was found that PDL can induce variations in the transmission spectrum, and affect the accuracy of the measured wavelength.

To verify the modeling results, experimental PDL measurements were carried out using the apparatus shown in Fig. 4. In these experiments, the bending radius was controlled by wrapping the fiber around a variable-diameter mandrel, as shown in Fig. 4. Input from a tunable laser was polarization-controlled, and the TE and TM responses were measured using an optical spectrum analyser and associated data-collection software.

As mentioned above using a scalar approximation of the wave equations for the analysis of light propagation in singlemode fiber, values of macrobending loss for the TE and TM modes are calculated as a function of bend radius and are presented in Fig. 5(*a*), while their difference value is shown in Fig. 5(*b*). The differences between calculated TE and TM mode bend losses are largest at the bend radii of 9.2 and 11.3 mm. Measured values are also shown and are generally in reasonable agreement with the calculated result. Occasional discrepancies between experimental and theoretical results in Fig. 5(*b*) are most likely caused by inaccuracy in measuring the bending radius and/or approximations made in calculating bend loss.

Fig. 6 shows the measured PDL values for 1060XP fiber at a 10.5 mm bend radius (single-turn); calculated results (using the correction factor obtained at 1550nm) are also shown. As mentioned in Sec. 2, PDL calculations employed correction factors at a limited number of wavelength intervals (10 nm) across the wavelength range 1500-1600 nm. Within this range, calculated and experimental results are in semi-quantitative agreement (with some random variations in the experimental data). The calculated results agree with experimental values more closely at 1500-1550 nm than at 1550-1600 nm. The discrepancy between the calculated PDL and measured results could be caused by approximations made in the calculations and/or by imperfect absorbing layer material coated on the fiber surface. If this layer does not absorb all the radiation from the core at the bend then some partial radiation will reflect from the fiber coating-air boundary and recouple with the fundamental propagation mode, resulting in changes to the polarization states of the fundamental mode.

4. PDL of bare bent 1060XP fiber with an absorbing layer

According to the boundary equations (3) and (4), a stripped bare 1060XP fiber with an absorbing layer (q=1, 2), can be treated as a fiber core-infinite cladding structure, and the calculated PDL is virtually zero at a bend radius of 10.5 mm.

In the experiment, the bare fiber section coated with an absorbing layer using acrylic based material was bent to form a small 360^o loop in free space, with the bare fiber loop cross section protected by a polymer jacket for mechanical stability. The fiber ends were connected to a polarization controller and an optical spectrum analyzer, respectively. The measurement was undertaken as described in Sec. 3.

Experimental PDL values for bare 1060XP fiber with an absorbing layer are presented in Fig. 7. For comparison, measured PDL values for 1060XP fiber with coating and absorbing layers are also shown. PDL values for coated fiber are in general greater than for bare fiber. In Fig. 7, as mentioned in Ref. [7], the divergences between the experimental and theoretical PDL results for bare 1060XP fiber are most likely caused by imperfect in the absorbing layer material. In the PDL measurements, it should be noted that there is about 0.02 dB variation exists in the wavelength measurements due to the Signal-Noise-Ratio (SNR) of the tunable laser source, and it effects the polarization dependent loss measurement result as well. Overall we can conclude that the use of bare 1060XP fiber, for the implementation of a compact single-turn fiber edge filter, has a significantly better PDL performance by comparison with a 1060XP fiber with coating layer and absorbing layers.

5. Conclusion

In conclusion, both macrobending loss and PDL for bend loss sensitive fiber (1060XP) has been investigated theoretically and experimentally. Both theoretical and experimental results have shown that the coating layer has a significant influence on the polarization dependence of bend loss. It is suggested that the bent bare 1060XP fiber with an absorbing layer is more suitable for fiber bend loss edge filter applications.

Acknowledgement

The authors would like to thank Dr. Dan Kuehner for useful discussions and suggestions.

References

1. A. Mecozzi and M. Shtaif, The statistics of polarization-dependent loss in optical communication systems, IEEE Photon Technol Lett 14 (2002), 313-315.
2. R. M. Craig, Accurate Spectral Characterization of Polarization-Dependent Loss, J Lightwave Technol 21 (2003), 432-437.
3. L. Chen, Z. Zhang, X. Bao, Polarization dependent loss vector measurement in a system with polarization mode dispersion, Opt Fiber Technol 12 (2006), 251–254.
4. J. Q. Zhou, H. Dong, S. Aditya, Y.D. Gong, P. Shum, X. Guo, L. Ma, Two-states method for polarization dependent loss measurement, Opt Fiber Technol 13 (2007), 139–142.
5. Q. Wang, G. Farrell, T. Freir, G. Rajan and P. Wang, Low-cost wavelength measurement based on a macrobending single-mode fiber, Opt Lett 31 (2006), 1785-1787.
6. P. Wang, G. Farrell, Q. Wang and G. Rajan, An optimized macrobending-fiber-based edge filter, IEEE Photon Technol Lett 19 (2007), 1136-1138.
7. H. Renner, Bending losses of coated single-mode fibers: a simple approach, J Lightwave Technol 10 (1992), 544-551.
8. L. Faustini and G. Martini, Bend loss in single-mode fibers, J Lightwave Technol 15 (1997),

671-679.

9. Q. Wang, G. Farrell and T. Freir, Theoretical and experimental investigations of macro-bend Losses for standard single mode fibers, Opt Express 13 (2005), 4476-4484.
10. Y. Murakami and H. Tsuchiya, Bending losses of coated single-mode optical fibers, IEEE J Quantum Electron QE-14 (1978), 495-501.
11. A. B. Sharma, A. H. Al-Ani and S. J. Halme, Constant-curvature loss in monomode fibers: an experimental investigation, Appl Opt 23 (1984), 3297-3301.

Figure Captions:

Fig. 1 Cross section of bent fiber with core-cladding-infinite coating structure

Fig. 2 Calculated and measured macrobending loss for different bending radii at 1550 nm

Fig. 3 Correction factor as a function of wavelength.

Fig. 4 Schematic configuration of the experimental setup for PDL measurement

Fig. 5(a) Calculated bend loss for TE and TM mode for different bend radii (correction factor is 1.283 at 1550nm wavelength); (b) theoretical and experimental differences in bend loss between TE and TM mode for 1060XP fiber with different bend radii

Fig. 6 Experimental and calculated PDL values for fiber length of one turn and 10.5mm bend radius, across the wavelength range 1500-1600nm. (For calculated results, the correction factors measured which are presented in Fig. 3 are applied across this theoretical range.)

Fig. 7 Measured PDLs for bend radius of 10.5 mm (one turn)

Table Caption:

Table 1 Parameters of 1060XP fiber (refractive index values defined at 1550nm wavelength)

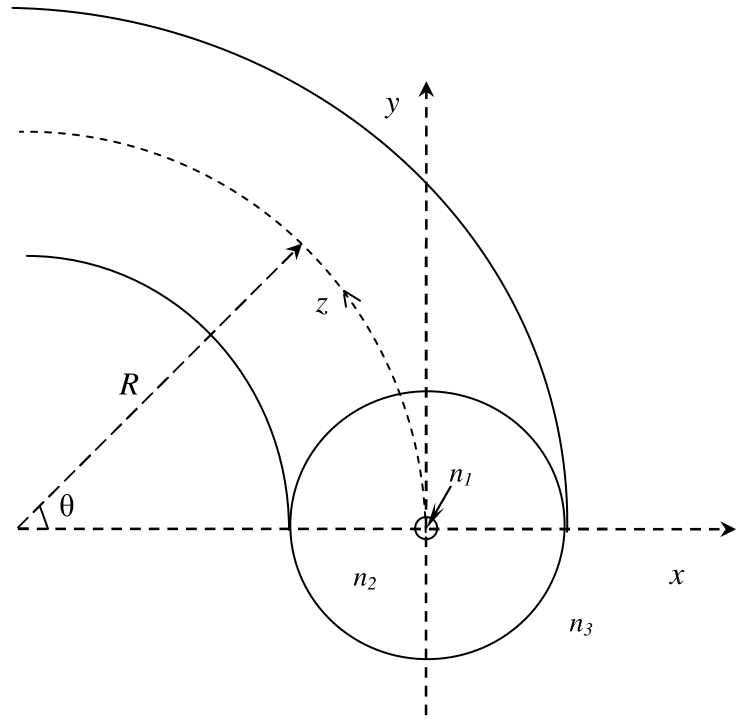

Fig.1 Cross section of bent fiber with core-cladding-infinite coating structure

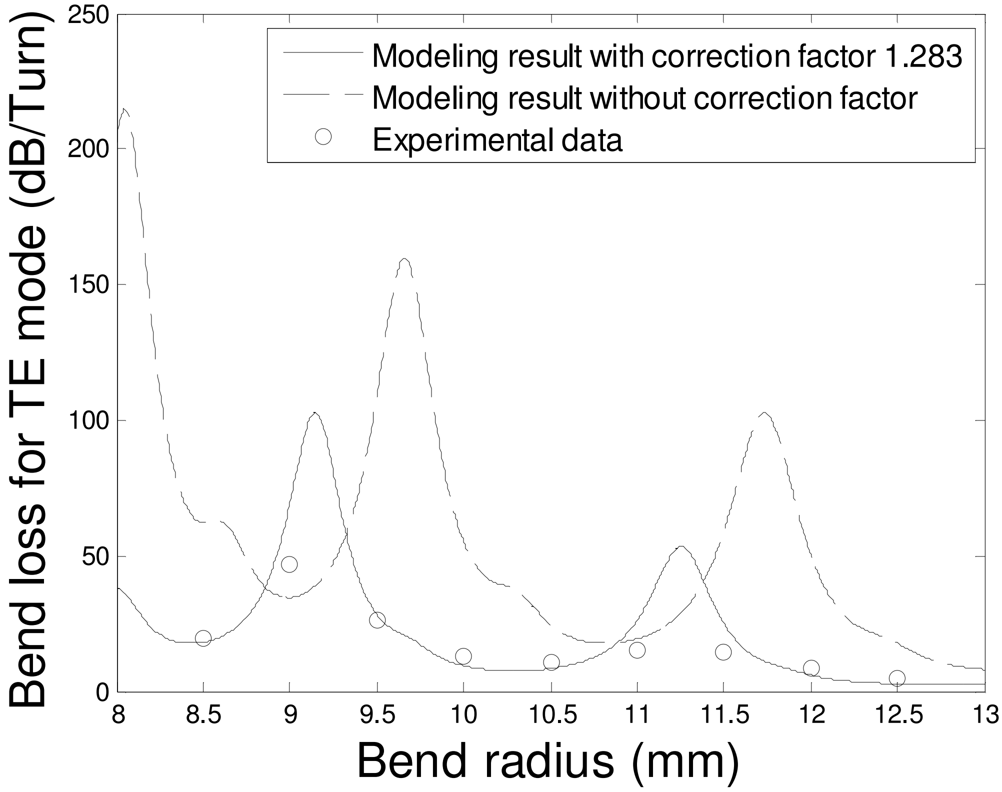

Fig. 2 Calculated and measured macrobending loss for different bending radii at 1550 nm

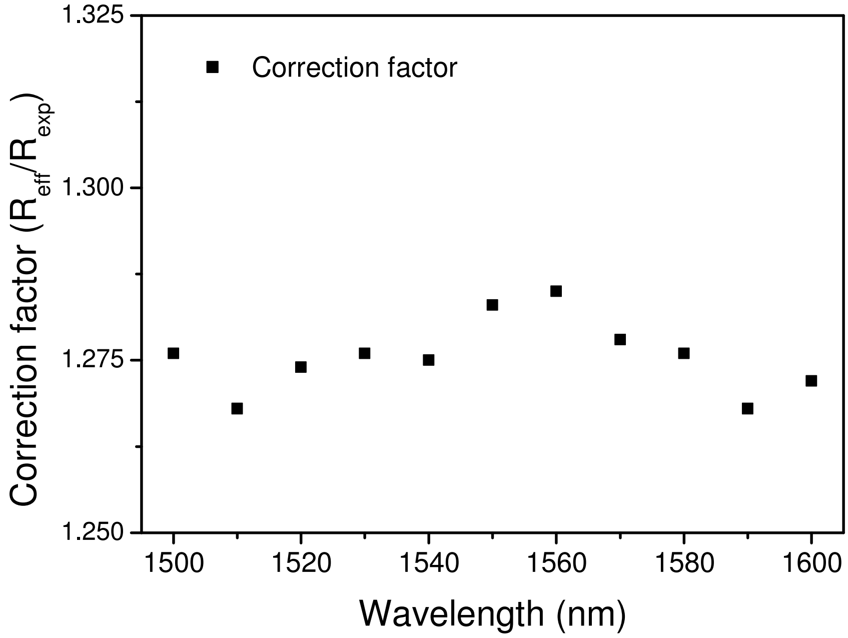

Fig.3 Correction factor as a function of wavelength.

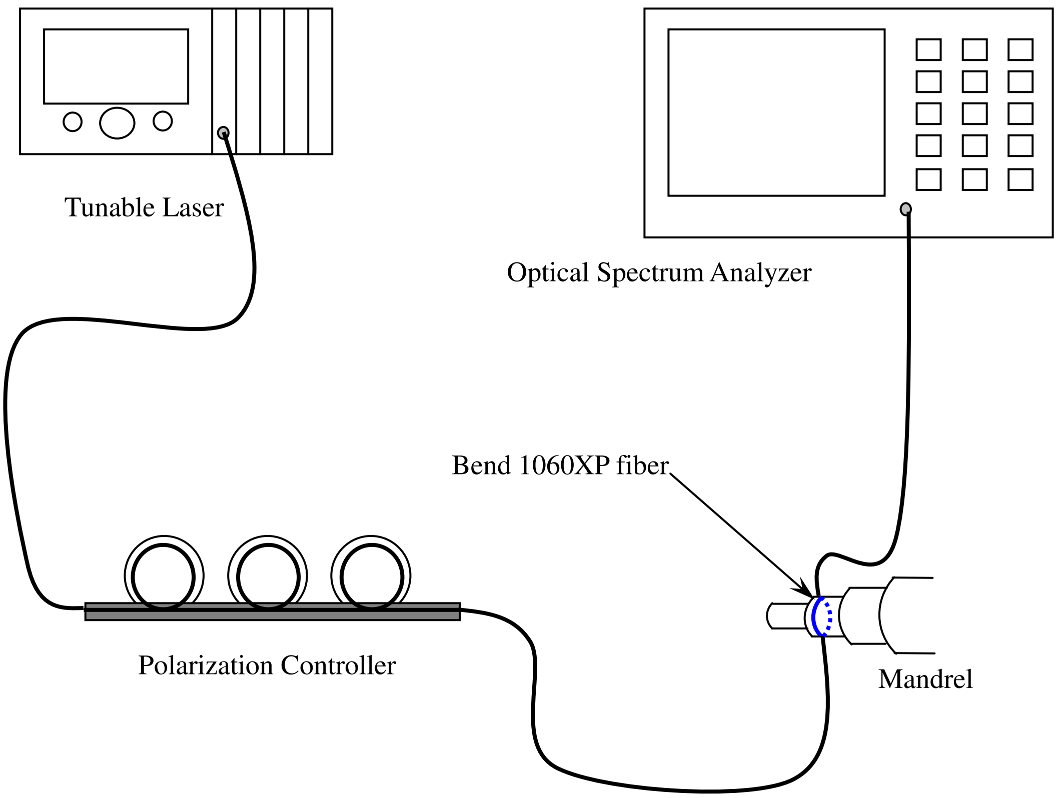

Fig. 4 Schematic configuration of the experimental setup for PDL measurement

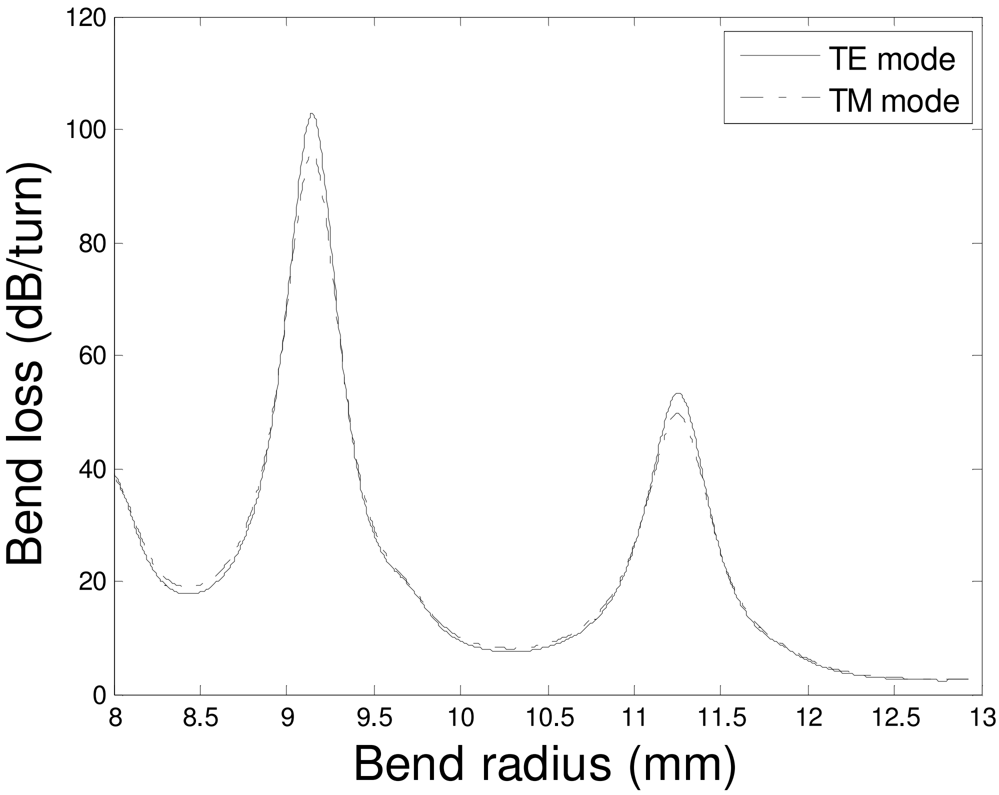
TE mode
TM mode
Bend loss (dB/turn)
Bend radius (mm)
0
20
40
60
80
100
120
8
8.5
9
9.5
10
10.5
11
11.5
12
12.5
13

(a)

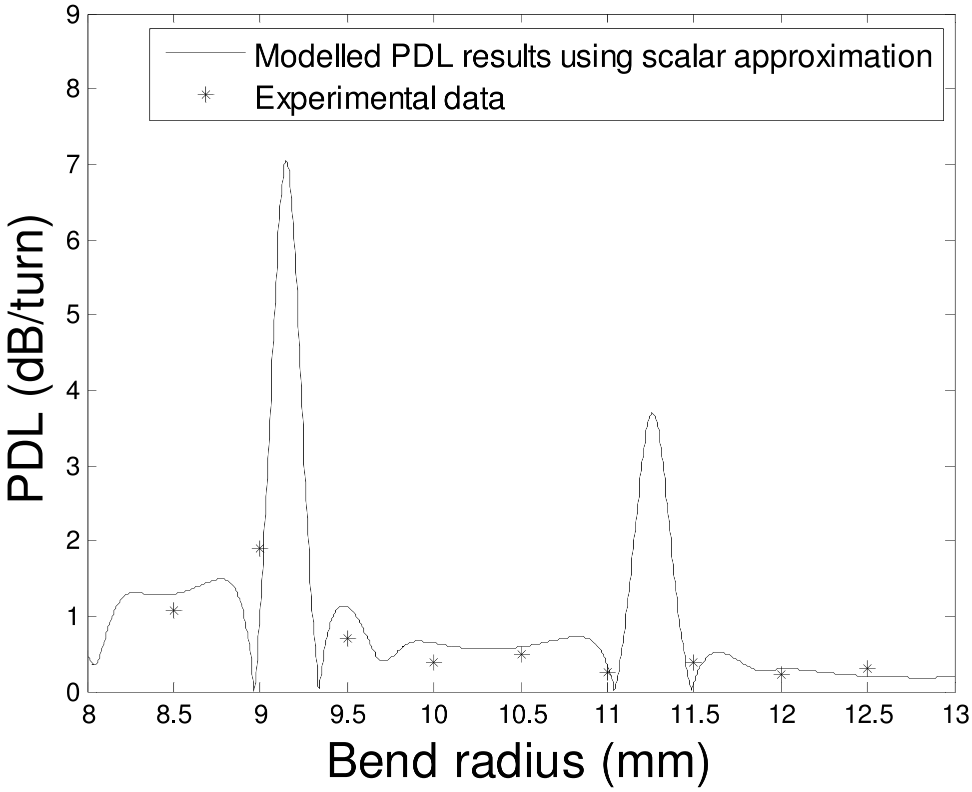

(b)

Fig. 5 (a) Calculated bend loss for TE and TM mode for different bend radii (correction factor is 1.283 at 1550 nm wavelength); (b) theoretical and experimental differences in bend loss between TE and TM mode for 1060XP fiber with different bend radii

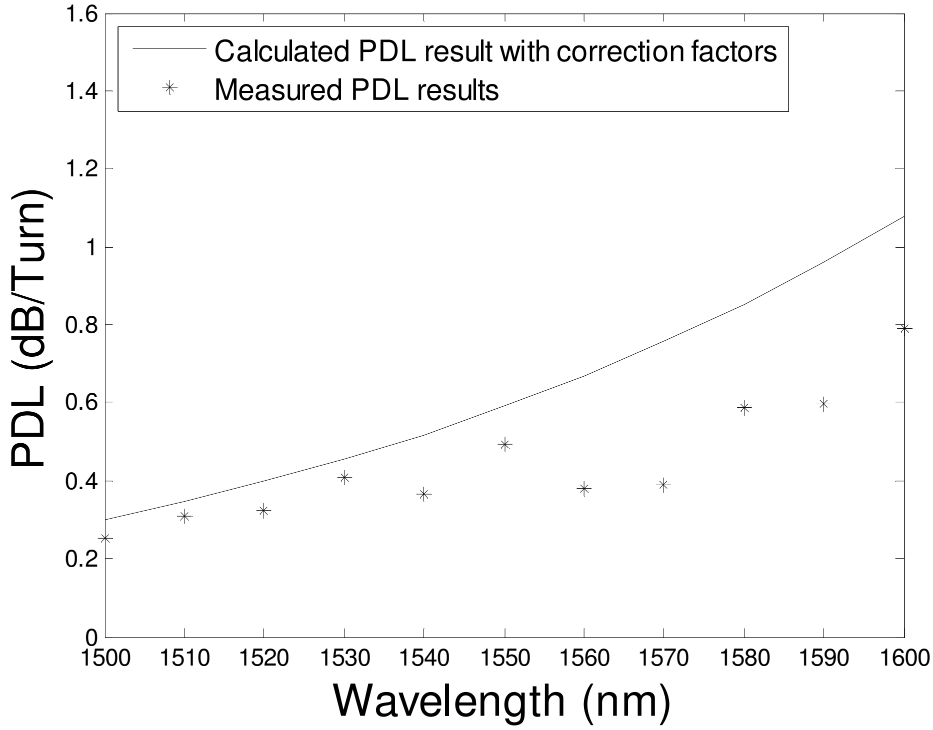

Fig. 6 Experimental and calculated PDL values for fiber length of one turn and 10.5mm bend radius, across the wavelength range 1500-1600nm. (For calculated results, the correction factors measured which are presented in Fig. 3 are applied across this theoretical range.)

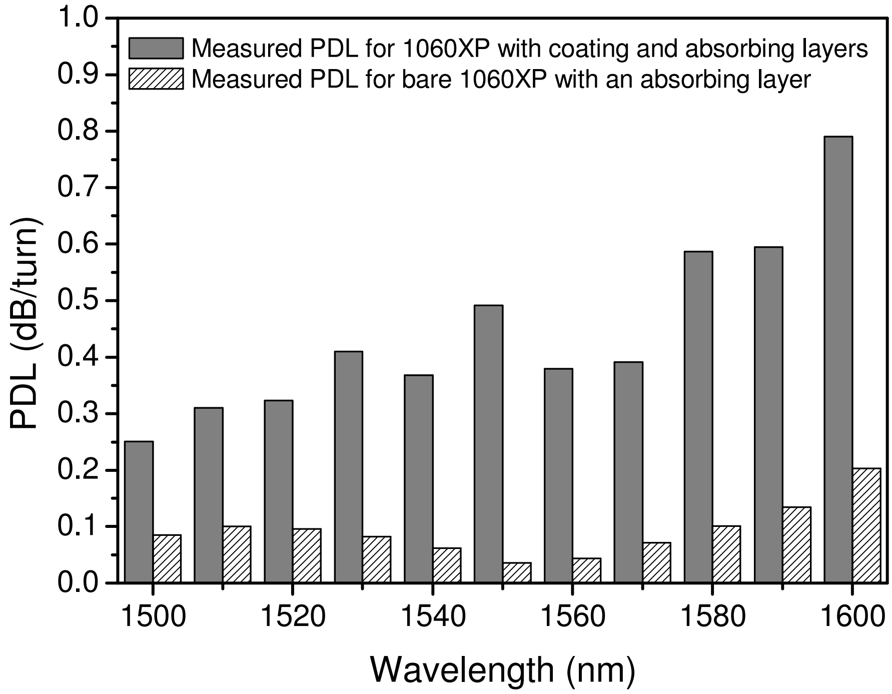

Fig. 7 Measured PDLs for bend radius of 10.5 mm (one turn)

Table 1 Parameters of 1060XP fiber (refractive index values defined at 1550nm wavelength)

Parameters of 1060XP fiber	
Refractive index difference (between fiber core and cladding)	0.0067
Refractive index of primary coating	1.4975
Refractive index of secondary coating	1.5068
Diameter of fiber core	5.3 ± 0.3 μm
Diameter of fiber cladding	125 ± 0.5 μm
Diameter of primary coating	195 μm
Diameter of secondary coating	245 μm
NA (Numerical Aperture)	0.14
V (Normalized frequency)	1.5035